Am J Transl Res 2020;12(1):292-307
www.ajtr.org /ISSN:1943-8141/AJTR0102563

Original Article

Human induced pluripotent stem cells ameliorate hyperoxia-induced lung injury in a mouse model

Adam Mitchell[1*], Heather Wanczyk[1*], Todd Jensen[1], Christine Finck[1,2]

[1]University of Connecticut Health Center, 263 Farmington Ave, Farmington, CT, USA; [2]Connecticut Children's Medical Center, 282 Washington St, Hartford, CT, USA. [*]Equal contributors.

Received September 20, 2019; Accepted January 3, 2020; Epub January 15, 2020; Published January 30, 2020

Abstract: Hyperoxia-induced lung injury occurs in neonates on oxygen support due to premature birth, often leading to the development of bronchopulmonary dysplasia. Current treatment options have limited effect. The aim of this study was to determine if human induced pluripotent stem cells (iPSCs) and those differentiated to an alveolar-like phenotype (diPSCs) could repair hyperoxia-induced lung damage in a mouse model. Neonatal C57BL6/J mice were separated into two groups and exposed to 75% oxygen over 6 or 14 days. Cell treatments were instilled intra-orally following removal. Controls included hyperoxia, normoxia, and a vehicle. 7 and 14 days post treatment, lungs were extracted and histomorphometric analysis performed. Gene expression of markers mediating inflammation *(Tgfβ1, Nfkb1, and Il-6)* were investigated. In addition, exosomes from each cell type were isolated and administered as a cell free alternative. There was a significant difference between the mean linear intercept (MLI) in hyperoxic vs. normoxic lungs prior to treatment. No difference existed between the MLI in iPSC-treated lungs vs. normoxic lungs after 6 and 14 days of hyperoxia. For mice exposed to 6 days of hyperoxia, gene expression in iPSC-treated lungs returned to normal 14 days later. At the same time points, diPSCs were not as effective. Exosomes were also not as effective in reversing hyperoxic lung damage as their cellular counterparts. This study highlights the potential benefit of using iPSCs to repair damaged lung tissue through possible modulation of the inflammatory response, leading to novel therapies for acute hyperoxia-induced lung injury and the prevention of bronchopulmonary dysplasia.

Keywords: Alveolar epithelial cell, Bronchopulmonary dysplasia, differentiated induced pluripotent stem cell, induced pluripotent stem cell, mesenchymal stem cell, post-natal, ventilator-induced lung injury

Introduction

Bronchopulmonary dysplasia (BPD) is a chronic respiratory illness that affects between 10,000-15,000 premature infants each year in the US [1]. Extremely premature infants (< 29 weeks) require early oxygen supplementation to support normal gas exchange. Often, hyperoxia-induced lung injury occurs and can lead to the development of BPD. BPD is initiated through the release of reactive oxygen species that cause damage to vital cellular constituents necessary for proper lung development [2, 3]. Current treatments such as antenatal corticosteroid and surfactant administration are not always effective and can fail to prevent long-term damage [4]. Studies have found that through early childhood, BPD has a negative impact on cognitive and neurodevelopmental outcomes along with decreased lung function [5]. Currently, no treatments exist that can reverse early hyperoxia-induced lung damage.

Cell therapies to address this clinical deficit have included mesenchymal stromal cells (MSCs), amnion epithelial cells and endothelial progenitor cells [6-9]. Based on rodent studies, these cells exert their effects through paracrine mechanisms, rather than direct engraftment within the lung [10-12]. MSCs from various sources can differentiate into multiple cell types and possess immunomodulatory properties [13, 14]. When administered in rodent models of BPD, MSCs attenuated inflammation, pulmonary hypertension and oxidative stress [15]. In one study, human umbilical cord blood-derived MSCs administered to neonatal rats exposed to hyperoxic conditions were able to improve alveolarization and fibrosis in damaged lungs by reducing the levels of cellular

apoptosis and cytokines responsible for inflammation [16]. Despite these beneficial effects, the clinical applicability of MSCs is reduced because they are heterogeneous cultures and have a limited lifespan *in vitro* after several passages [17]. Human induced pluripotent stem cells (iPSCs) are a potential alternative source for cell therapy because unlike MSCs they can proliferate almost indefinitely and are cultured as a relatively homogenous population. They can easily be generated from a patient's own somatic cells, such as peripheral mononuclear blood cells, dermal fibroblasts or epithelial cells and reprogrammed into a pluripotent state allowing for differentiation into various lineages such as cardiomyocytes, hepatocytes, neurons and cells of epithelial and alveolar origin [18, 19]. In response to ventilator-induced lung injury (VILI), iPSCs were able to suppress inflammatory and oxidative pathways [20, 21], suggesting a potential mechanism of action. Their antioxidant properties have also been demonstrated by high expression of proteins such as Glutathione (GSH) and also GSH-dependent enzymes [22-24].

The aim of our study was to assess whether iPSCs or iPSCs differentiated to an alveolar-like phenotype (diPSCs) could reverse hyperoxia-induced lung injury, potentially preventing the onset of BPD. The cells herein were differentiated to an alveolar-like phenotype based on previously published protocols [25-28]. We hypothesized that diPSCs may be beneficial because alveolar epithelial type II cells (AEC IIs), which the differentiated cells are intended to resemble, have the ability to proliferate and differentiate into alveolar epithelial type I cells (AEC I) post lung injury [29]. They are also responsible for surfactant production and are capable of self-renewal and immune modulation, making them an important component of normal lung growth and development [30, 31]. One study showed that addition of AEC II cells *in vitro* to a scratch damaged AEC II cell monolayer resulted in complete attachment and healing in a 24-hour period compared to undamaged monolayers, suggesting reparation by soluble autocrine factors [32]. Finally, diPSCs express few of genes responsible for teratoma formation, unlike their undifferentiated counterparts [33]. Exosomes were also isolated from both iPSCs and diPSCs and administered to mice to determine if they exhibited the same therapeutic potential as their cellular counterparts. Robustness of our model was ensured through the use of two hyperoxia exposures with follow up at 7 and 14 days.

Materials and methods

Cell preparation and implantation

iPSC generation, culture and differentiation was performed as previously described [34], outlined in **Figure 1A**. The human dermal fibroblasts used to generate the iPSCs were acquired with informed consent under Hartford Hospital IRB FINC00364HU. C57 BL/6J mice purchased from Jackson Laboratories (JAX stock #000664) were used throughout the study (IACUC 10124-118). Twenty-four hours after gestation, mother and pups were placed into a purpose-built cubicle, fed with O_2 and air, and allowed to equilibrate to ~75% O_2. Mice were checked daily and mothers rotated every 48 hours to prevent hyperoxia-induced damage to their lungs. One subset of mice (n=8-10 all groups) was kept in hyperoxic conditions for 6 days, while the other group remained under the same conditions for 14 days. Two different exposures were tested to ensure that sufficient lung damage was incurred. On the day of implantation (PN7 or PN15), cells were washed twice with PBS and dissociated in TrypLE™ Express (ThermoFisher Scientific, Grand Island, NY) for 5 minutes. Cells were then centrifuged at 300 g for 5 minutes, counted on a hemocytometer and 1×10^5 cell were re-suspended in 40 µL aliquots of Hanks Balanced Salt Solution (HBSS) without Ca^{2+} (ThermoFisher Scientific). Aliquots were pipetted into the oral cavity and the pups encouraged to aspirate the fluid by gently pinching the end of the tail. Previous studies have shown that intraoral administration of cells is nearly as effective as intratracheal administration, but the process is far less invasive and causes less distress to the animal [35]. HBSS alone was used as a vehicle control. Post recovery, the mother and pups were returned to normal atmospheric conditions for 7 or 14 days, after which the pups were euthanized by CO_2 exposure and the lungs removed. Finally, on alternating postnatal days from P1 to P15, pups (n=3-4) were euthanized and the lungs collected to assess changes in gene expression as a result of the hyperoxic conditions. Intraoral delivery of iPSCs to the mouse lungs was confirmed by staining with CellBrite™ Fix (Biotium, Freemont, CA). Cells were stained for 15 minutes at 37°C according

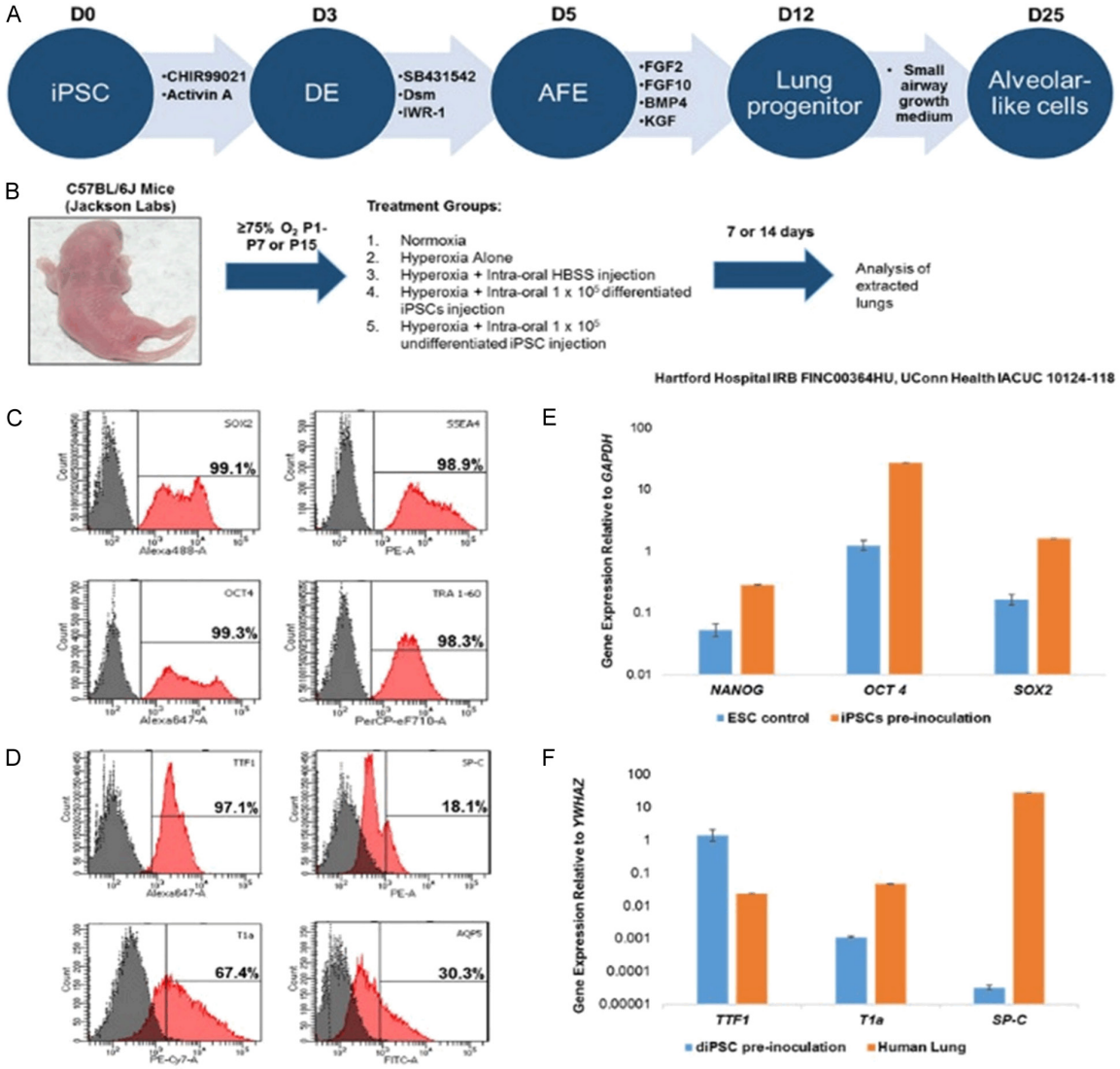

Figure 1. Experimental design and representative phenotype of the undifferentiated and differentiated iPSCs used for implantation. A. Schematic representation of the differentiation of iPSCs to an alveolar-like phenotype. The cells used in the study were from D0 and D25. B. Experimental groups for hyperoxia induced lung damage. Normoxia, hyperoxia and hyperoxia plus Hank's Balanced Salt Solution (HBSS) vehicle were included as controls. C. Flow cytometry showed a >98% expression of the iPSC markers OCT4, SOX2, SSEA4 and TRA-1-60. E. qRT-PCR analysis of iPSC marker expression prior to inoculation, included is the expression in embryonic stem cells as a comparison. D. Flow cytometry showed 97.1% and 67.4% expression of differentiated iPSC markers TTF1 and T1a, along with 30.3% AQP5 and 18.1% SP-C expression. F. qRT-PCR analysis of diPSC marker expression prior to inoculation. Human adult lung was used as a positive control. Gene expression for markers *TTF1*, *T1a* and *SP-C* was detected in all cells.

to manufacturer's instructions (Figure S2) and administered at 100,000 cells/pup in HBSS. Mice were euthanized an hour later, the lungs excised and prepared for histology.

Flow cytometry and qRT-PCR analysis of iPSC and diPSCs

For flow cytometry analysis, cells were first washed twice in PBS then dissociated using TrypLE™ (ThermoFisher Scientific), for 5 minutes at 37°C. Cells were then centrifuged at 300 g for 5 minutes, re-suspended in HBSS without Ca^{2+} (ThermoFisher Scientific) and incubated with fixable viability dye eFluor 780 (eBioscience, San Diego, CA) for 30 minutes at 4°C. Following this, cells were centrifuged at 300 g for 5 minutes and fixed in 4% paraformaldehyde (PFA) for 5 minutes. iPSCs were stained with the following antibodies/fluorophores, OCT4/e660, SOX2/A488, SSEA4/PE and TRA-1-60/PerCP eF710 (all eBioscience)

Table 1. List of conjugated antibodies used in flow cytometry

Marker	Differentiation Phase	Fluorophore	Manufacturer/Catalogue number
OCT 4	iPSC	e660	eBioscience/50-5841-82
SSEA4	iPSC	PE	eBioscience/12-8843-41
TRA-1-60	iPSC	PerCP eF710	eBioscience/46-8863-82
SOX2	iPSC	A488	eBioscience/53-9811-82
SP-C	diPSC	PE	Bioss/bs-10067R
T1α	diPSC	PE-CY7	Biolegend/337014
TTF1	diPSC	A647	Bioss/bs-0826R
AQP5	diPSC	FITC	Bioss/bs-1554R
CD63	Exosome	PE	BD Biosciences/557305
CD81	Exosome	PerCP eF710	eBioscience/46-0819-41

Table 2. List of primers used for qRT-PCR analysis

Gene	Assay Number	Manufacturer
OCT 4	Hs04260367	Thermofischer Scientific
NANOG	Hs04399610	Thermofischer Scientific
SOX2	Hs01053049	Thermofischer Scientific
GAPDH	Hs99999905	Thermofischer Scientific
SP-C	qHsaCEP0057801	Bio-Rad
T1α	qHsaCIP0027018	Bio-Rad
TTF1	qHsaCEP0051347	Bio-Rad
Il-6	qMmuCEP0054186	Bio-Rad
Tgfb1	qMmuCEP0053152	Bio-Rad
Nfkb1	qMmuCEP0055648	Bio-Rad
B2M	qHsaCIP0029872	Bio-Rad
YWHAZ	qHsaCIP0029093	Bio-Rad
GAPDH	qMmuCEP0039581	Bio-Rad

in PBS containing 2% fetal bovine serum (FBS) and 0.1% Triton X-100 (only for antibodies with intracellular targets) for 30 minutes at 4°C (**Table 1**). The same protocol was followed for diPSCs, but the antibodies/fluorophores used were as follows; AQP5/FITC, SPC/PE, TTF1/A647 (Bioss, Woburn, MA), T1α/PE-CY7 (Biolegend, San Diego, CA). Samples were then filtered, and flow cytometry analysis was performed on an LSR II (BD Biosciences, San Jose, CA). Machine compensation was performed using unstained cells, viability dye stained cells and UltraComp ebeads (eBioscience) conjugated with each antibody. Dead cells and debris were gated out and histograms drawn displaying the detection of each antibody in live cells and an unstained control overlaid with the percentage of stained, live cells calculated.

For qRT-PCR analysis of iPSCs and diPSCs administered to mice, 350 μL of RLT lysis buffer was added to cells. Using a RNeasy Plus Mini Kit (Qiagen, Waltham MA), genomic DNA was removed with gDNA eliminator columns followed by RNA isolation performed according to manufacturer's instructions. Isolated RNA was then reverse transcribed into cDNA using an iScript Reverse Transcription Supermix for RT-qPCR (Bio-Rad, Hercules CA). Genes used to characterize iPSC cells were *NANOG*, *OCT4*, and *SOX2* (ThermoFisher Scientific). Human embryonic stem cell H9 total RNA was used as the positive control (ScienCell Research Laboratories, Carlsbad, CA). diPSC characterization was performed using the following genes; *TTF1*, *T1α* and *SP-C* (Bio-Rad), with total RNA from human adult lung serving as the positive control (BioChain Institute, Newark, CA). PCR plates were run using a CFX96 Real-Time System from Bio-Rad, primer assay numbers are listed in **Table 2**. Data was analyzed using the ΔCT method with *GAPDH* and *YWHAZ* as the endogenous controls.

Analysis of lungs prior to and after cell delivery

Lungs from pups (n=3) in each test group were removed at the appropriate time points and fixed in 4% paraformaldehyde overnight at 4°C. The following day, fixed lungs were transferred to 70% ethanol and sent to the University of Connecticut Histology Core to be paraffin embedded, sectioned and stained with Hematoxylin and Eosin. Six random lung sections from the upper, middle and base of the lung were imaged from each animal at 20 × magnification using a Zeiss Observer Z1 inverted bright field/fluorescence microscope running Zen Blue software. The mean linear intercept (MLI) was calculated based on a previous study [36], whereby a lower MLI value corresponded to a greater degree of lung damage. Histological images were uploaded to ImageJ and overlaid with equally spaced line segments. The number of times a line intersected an alveolar wall was quantified and the average from each group determined. All counting was done blind and statistical significance was determined by one-way ANOVA and

Table 3. List of antibodies used for immunofluorescence

Antibody	Host	Manufacturer/Catalogue number
TGFβ1	Rabbit	Abcam/ab92486
MMP2	Rabbit	Abcam/ab37150
IL-6	Rat	ThermoFisher Scientific/MM600C
2° Ab Goat anti-Rabbit 488	Goat	ThermoFischer Scientific/A11008
2° Ab Goat anti-Rat 546	Goat	ThermoFischerScientific/A11081

Table 4. List of antibodies used for Western blot

Antibody	Manufacturer/Catalogue number
Exosome-anti-CD81	Thermofischer Scientific/10630D
Exosome-anti-CD63	Thermofischer Scientific/10628D

Bonferroni post-test using GraphPad Prism with P<0.05 considered significant, with data displayed as box and whisker plots.

Lungs (n=3-4 each test group) were homogenized using a bead mill (ThermoFisher Scientific) and subsequently RNA was isolated and cDNA prepared as described above. qRT-PCR was used to detect the expression of genes responsible for inflammation (*Il-6*, *Tgfβ1*, *Nfkb1)* and matrix degradation/deposition *(Col-1a1, Mmp2),* primer assay numbers can be found in **Table 2**. Genes were chosen based on the following published studies [37-41]. qRT-PCR plates were run using a CFX96 Real-Time System. Data was analyzed using the ΔCT method with *B2m* or *Gapdh* as the endogenous control.

Lung samples from each group that had been previously embedded and sectioned were prepared for immunofluorescent staining. Antigen retrieval was performed using a 0.05% working solution of Trypsin/EDTA at 37°C, pH 7.8 for 20 minutes (Thermofisher Scientific). Tissue samples were washed twice with PBS and then blocked and permeabilized in PBS, containing 0.1% Tween, 0.1% Triton X-100 and 2% FBS for 45 minutes. Samples were then stained with the following antibodies, MMP2, TGFβ1 (both Abcam, Cambridge, UK), and IL-6 (ThermoFisher Scientific) at a 1:100 dilution in the blocking solution used above, at 4°C overnight (See **Table 3**). The following day, samples were rinsed twice with PBS and stained with the following secondary antibodies, Goat anti-Rabbit 488 and Goat anti-Rat 546 (both ThermoFisher Scientific) at a 1:500 dilution in PBS and incubated at room temperature for 1 hour. Sections were then rinsed twice in PBS, stained with DAPI at room temperature for 10 minutes, followed by a final rinse in PBS. Samples were imaged using a Zeiss Observer Z1 inverted bright field/fluorescence microscope running Zen Blue software at 10 × magnification.

Statistical analysis

Statistical significance was determined by one-way ANOVA and Bonferroni Multiple Comparison Test using GraphPad Prism with P< 0.05 considered significant.

Isolation characterization and delivery of exosomes derived from iPSCs and diPSCs

Approximately 12 mL of cell culture medium supernatant from each cell type was collected, centrifuged at 2,000 g for 30 minutes to remove any cells and the supernatant mixed with 6 mL of Total Exosome Isolation Reagent (Thermofisher Scientfic). Samples were then incubated at 4°C overnight. The following day, samples were centrifuged at 12,000 g for 60 minutes. The supernatant was then removed, and the extracellular vesicle pellet resuspended in 1 mL of 0.1% BSA + PBS. Exosomes were purified by incubating with CD63 and CD81 antibody conjugated superparamagnetic Dynabeads (Thermofisher Scientific) per manufacturer's instructions. Exosomes were characterized and sorted using flow cytometry and their contents analyzed by Western Blot. For flow cytometry, Dynabead conjugated exosomes were incubated with anti-CD63-PE (and anti-CD81-PerCP-eF710 for 30 minutes at room temperature (See **Table 4**). Excess antibody was washed out by magnetizing the bead/exosome complexes which were then suspended in PBS containing 2% FBS and sorted on a BD FACs Aria II. An unstained bead/exosome sample was used as a negative control and only exosome/bead complexes positive for both CD63 and CD81 collected.

Scanning electron microscopy was used to visualize exosomes that had been conjugated to Dynabeads and sorted by flow cytometry. To prepare the samples 5 µl of either unconjugated Dynabeads or sorted exosome/bead complexes was allowed to evaporate on a silicon wafer for 1 hour at room temperature then coated in gold and analyzed on a JEOL-JSM-5900 LV scanning electron microscope.

Following sorting, 75,000 exosome/bead complexes were suspended in 40 µl HBSS and delivered to animals intraorally as previously described.

For Western Blot, CD81 and CD63 Dynabead conjugated exosomes were solubilized with a mix of 10 uL RIPA buffer and a 1:100 dilution of protease inhibitors (Roche Diagnostics, San Francisco, CA). Samples were then sonicated for 10 seconds and incubated on ice for 15 minutes. 3 uL of 5X sample buffer were added to each sample and incubated at 95°C for 5 min, loaded onto a 12% gel and run at 100 V for 1 hr. A wet transfer using a PVDF membrane was then performed at 100 V for 1 hr on ice, followed by blocking for 1 hr in nonfat milk (Biorad). Samples were incubated overnight at 4°C with a 1:250 dilution of exosome-anti-CD63 or exosome-anti-CD81 antibody (Thermofisher). The following day, samples were rinsed twice with wash buffer, incubated with a 1:1000 dilution of an anti-mouse HRP-conjugated secondary antibody (Sigma) for 1 hr and then rinsed again. Antibody-antigen complexes were identified by chemiluminescence (ECL + System, Amersham Biosciences, Piscataway, NJ), and imaged using a Chemi-Doc™ MP Imaging System from Biorad.

Results

Analysis of undifferentiated and differentiated iPSC phenotype

The cells used in this study were undifferentiated iPSCs and iPSCs differentiated to an alveolar-like phenotype as outlined in **Figure 1A**. Both cell types were analyzed for the expression of the appropriate markers to ensure they were of the expected phenotype. It was found that >98% of undifferentiated iPSCs expressed the markers OCT4, SOX2, SSEA4 and TRA-1-60 (**Figure 1C**) as measured by flow cytometry. qRT-PCR analysis of iPSCs confirmed appropriate marker expression (**Figure 1E**).

Following 25 days of differentiation and just prior to implantation, diPSCs were tested for the expression of alveolar type I (AQP5 and T1α) and alveolar type II (SP-C and TTF1) markers. The expression of alveolar type I markers was 30.3% and 67.4% (AQP5 and T1α respectively) and the expression of alveolar type II markers 18.1% and 97.1% (SP-C and TTF1 respectively) (**Figure 1D**). qRT-PCR analysis of the diPSCs confirmed the expression of *TTF1*, *T1α* and *SP-C* (**Figure 1F**). Gene expression from normal human adult lung was used as a positive control.

Histomorphometric analysis of iPSC treated mouse lungs following hyperoxia-induced lung damage

At P1, C57BL/6J mice were exposed to 75% O_2 over a total of 14 days to induce hyperoxic lung injury that predates BPD. There was a significant difference in the MLI of the hyperoxia group compared to the normoxic group prior to treatment ($P<0.001$) (**Figure 2A**). Representative H&E staining of the lung samples revealed substantial alveolar simplification in the hyperoxic group (**Figure 2B**). At 7 and 14 days post treatment, lungs were analyzed to assess the degree of damage/repair that occurred. As seen with mice exposed to 6 days of hyperoxia, there was a statistically significant difference in the MLI between normoxic vs. hyperoxic samples and normoxic vs. HBSS samples at day 7, $P<0.001$ (**Figure 2C**). There was also a statistically significant difference in the MLI between hyperoxic vs. iPSC-treated samples, $P<0.001$. There was no difference seen in the MLI of iPSC-treated lungs vs. the normoxic group and the hyperoxic group vs. HBSS control (**Figure 2C**). H & E staining indicated the presence of increased alveolar simplification in both the hyperoxic and HBSS groups. When compared to the normoxic sample, lungs treated with the two cell types exhibited less simplification overall (**Figure 2D**). At 14 days post treatment, there was a significant reduction in MLI between normoxic vs. hyperoxic, $P<0.001$, normoxic vs. HBSS, $P<0.001$ and normoxic vs. diPSCs, $P<0.01$. The MLI of the iPSC-treated group was statistically the same as the normoxic group. There was also a significant difference in the MLI of the hyperoxic vs. iPSC-treated group, $P<0.001$ (**Figure 2E**). Representative H & E staining of the 14-day samples revealed that iPSC treated lungs had a similar morphology to that of the normoxic group. diPSC treated lungs had a morphology comparable to that of HBSS treated and hyperoxic lungs (**Figure 2F**). When mice were exposed to shorter duration of hyperoxia (6 days), similar trends were observed (Figure S1).

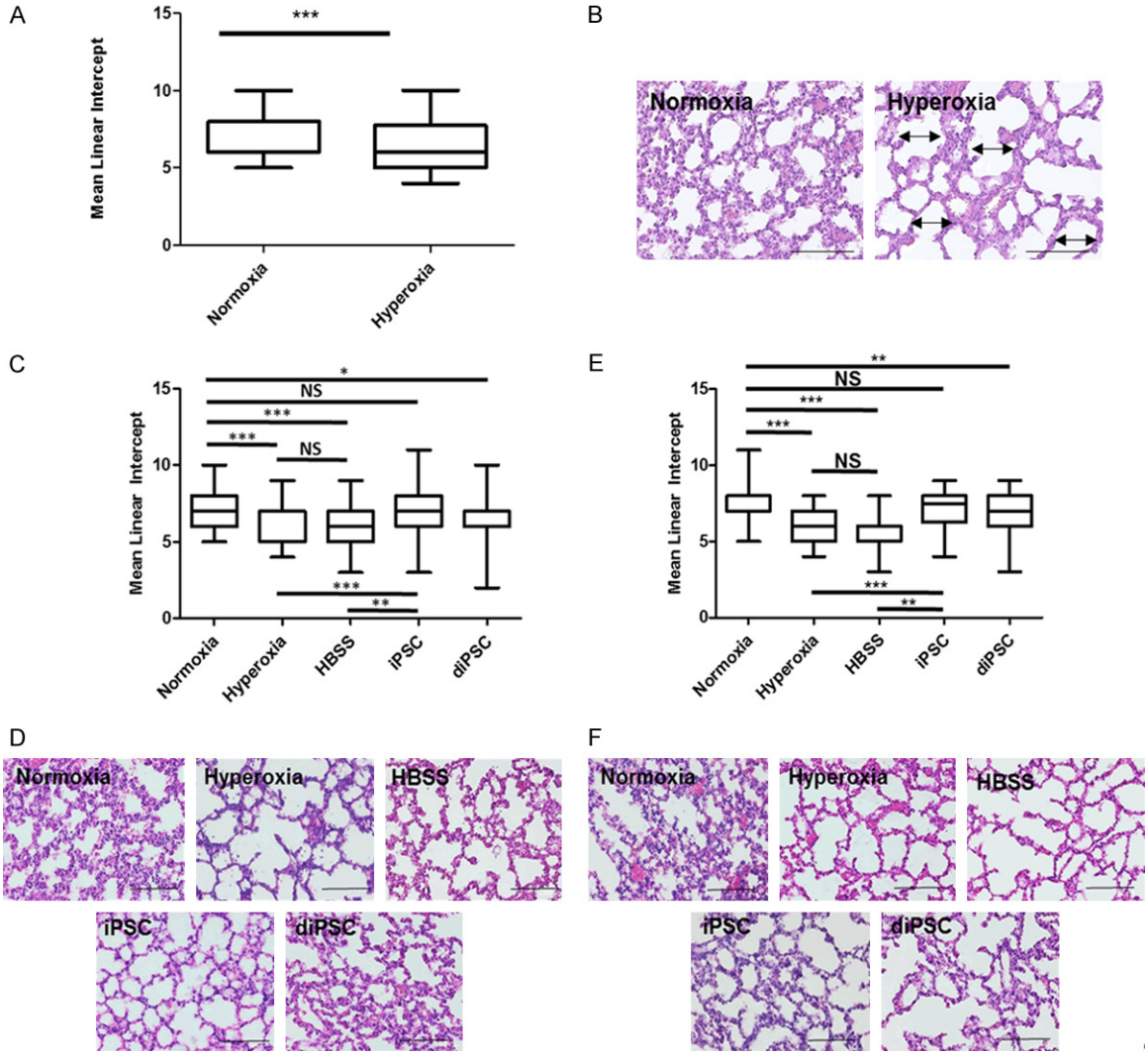

Figure 2. Histomorphometric data of C57 BL/6 mouse lungs following 14 days of hyperoxia induced lung damage. A, C, E. Mean linear intercept values for all groups. A. Post-natal Day 15. There was a statistically significant difference between normoxia vs. hyperoxia, P<0.001. C. 7 days post cell treatment. Across all groups the statistically significant differences were seen in normoxia vs. hyperoxia, P<0.001 normoxia vs. HBSS, P<0.001 hyperoxia vs. iPSC, P<0.001 HBSS vs. iPSC, P<0.01 normoxia vs. diPSC, P<0.05. There was no statistical difference between normoxia vs. iPSC and hyperoxia vs. HBSS. *P<0.05, **P<0.01, ***P<0.001 between indicated groups. E. 14 days post cell treatment. The result was exactly the same as 7 days post cell treatment with one exception, a significant difference between normoxia and diPSC, P<0.01. B, D, F. Representative H + E staining of all groups, each image has the MLI closest to the group mean, scale bars 50 μm. B. Post-natal Day 15. The presence of alveolar simplification is indicated by double-sided arrows and septal thickening by single-sided arrows. D. 7 days post cell treatment. F. 14 days post cell treatment.

Expression of hyperoxia-associated genes following hyperoxia exposure

To further determine the effects of each cell treatment on mice lungs exposed to hyperoxic conditions, the expression of *Tgfβ1*, *Nfkb1,* and *Il-6* was analyzed. At 7 days post treatment in mice exposed to 6 days of hyperoxia, there was a significant reduction in *Tgfβ1* expression in lungs treated with diPSCs vs. those treated with iPSCs, P<0.01 (**Figure 3A**). There was also a significant difference in *Il-6* expression between the two groups, P<0.05, and between the normoxic group and iPSC treated group (**Figure 3A**).

At day 14 post-treatment (**Figure 3B**), *Il-6* expression was significantly increased in hyper-

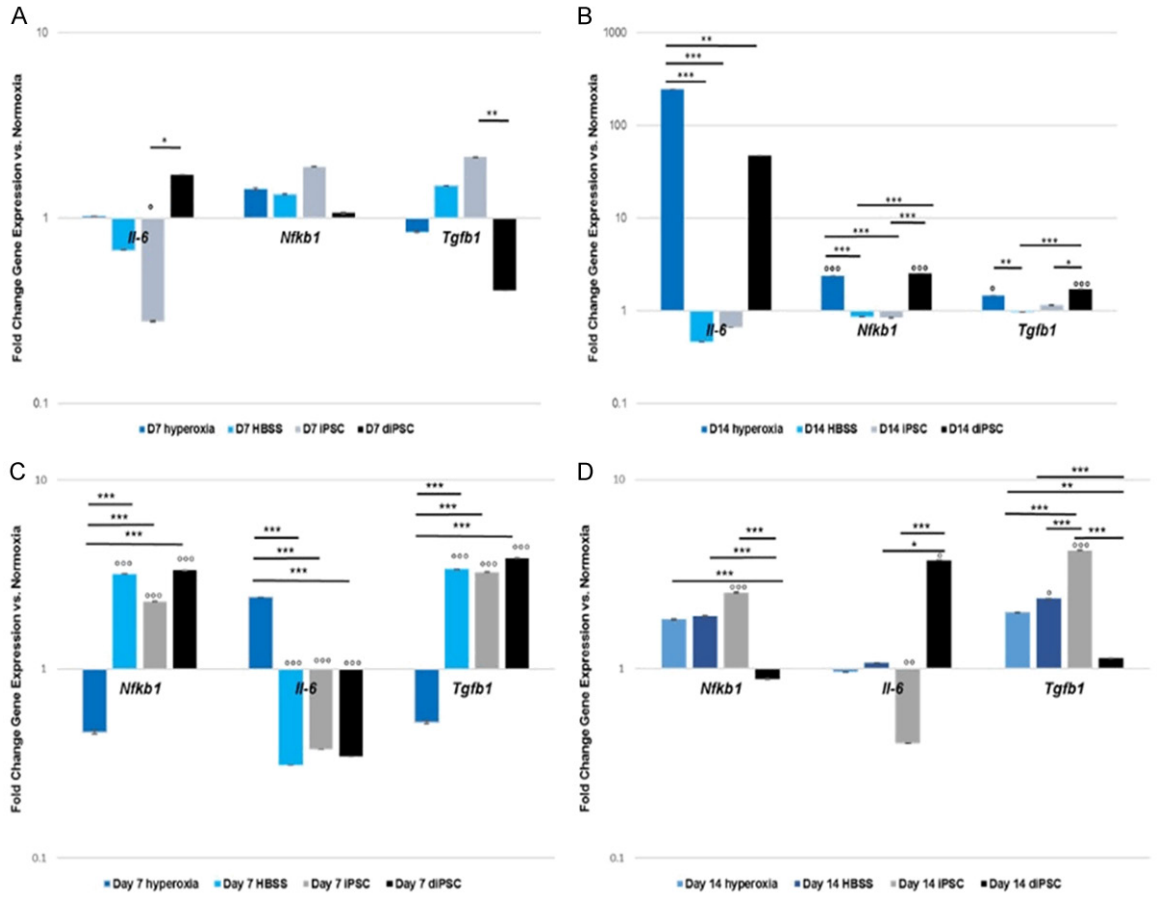

Figure 3. Gene expression over 7 and 14 days of hyperoxia induced lung damage in C57 BL/6 mice, Hyperoxic vs. Normoxic lung samples. A. Nfkb1, Il-6 and Tgfβ1 gene expression 7 days post cell treatment. There was a statistically significant difference between lungs treated with iPSC vs. diPSC in regards to *Tgfβ1* expression, P<0.01. There was also a statistically significant difference in *Il-6* expression between the iPSC treated group and the normoxia and diPSC-treated groups P<0.05. B. *Nfkb1, Il-6 and Tgfβ1* gene expression 14 days post cell treatment. *Il-6* expression, there was a significant difference between the hyperoxia alone group and all others P<0.01-P<0.001. *Tgfβ1* expression, there was a significant difference between normoxia and both the hyperoxia P<0.05 and diPSC-treated groups P<0.001, the hyperoxia and HBSS-treated group, P<0.01, and finally between the diPSC treated group and both the HBSS group, P<0.001 and iPSC group, P<0.05. Lastly, *Nfkb1* was significantly increased in the hyperoxia alone and diPSC treated groups compared with the normoxia control, P<0.001 and also compared with the HBSS and iPSC treated groups P<0.001. °P<0.05, °°P<0.01, °°°P<0.001 between the indicated group and the normoxia control, *P<0.05, **P<0.01, ***P<0.001 between the indicated groups. C. *Nfkb1, Il-6 and Tgfβ1* gene expression 7 days post cell treatment. There was a statistically significant difference between hyperoxia alone and lungs treated with iPSCs, diPSCs and HBSS in regards to *Nfkb1, Il-6 and Tgfβ1* expression, P<0.001. All groups were also significantly different from normoxia, with the exception of hyperoxia, P<0.001. D. *Nfkb1, Il-6 and Tgfβ1* gene expression 14 days post cell treatment. *Il-6* expression, there was a significant difference between diPSC-treated lungs vs. iPSCs, P<0.001 and diPSC-treated lungs vs. HBSS, P<0.05. Differences were also seen in iPSC-treated lungs vs. normoxia, P<0.01 and diPSC-treated vs. normoxia, P<0.05. *Tgfβ1* expression, there was a significant difference between normoxia and both the HBSS P<0.05 and iPSC-treated groups P<0.001. Expression was increased in iPSCs vs. HBSS, hyperoxia and diPSC-treated lungs, P<0.001. There were significant differences between diPSCs vs. hyperoxia, (P<0.01) and HBSS (P<0.001) treated groups. Lastly, *Nfkb1* was significantly increased in the iPSC-treated lungs vs. the normoxic group (P<0.001) and diPSC-treated lungs (P<0.001). There was also a significant difference in the diPSC-treated group vs. HBSS and hyperoxia, P<0.001. °P<0.05, °°P<0.01, °°°P<0.001 between the indicated group and the normoxia control, *P<0.05, **P<0.01, ***P<0.001 between the indicated groups.

oxia vs. all other groups (P<0.01-P<0.001). *Nfkb1* and *Tgfβ1* expression was significantly elevated in both the hyperoxic group and diPSC treated lungs compared with mice in normoxic conditions (P<0.05-P<0.001). In addition, the expression of *Nfkb1* was significantly increased

in the hyperoxia and diPSC treated groups compared with the HBSS and iPSC treated groups (P<0.001). Similarly, the expression of *Tgfβ1* was significantly increased in the hyperoxia and diPSC treated groups compared with the HBSS and iPSC treated groups (P< 0.05-P<0.001). There were no significant differences in expression of all markers between the normoxic group, vehicle control or the iPSC treated lungs (**Figure 3B**).

As with the shorter O_2 exposure, the same gene expression analysis was conducted on samples that underwent the longer O_2 exposure. At 7 days post treatment there was a significant difference between hyperoxia alone and lungs treated with iPSCs, diPSCs and the HBSS for all genes tested, P<0.001 (**Figure 3C**). Gene expression across all markers in each group was also significantly different when compared to the normoxic group, P<0.001 (**Figure 3C**).

At day 14 post-treatment (**Figure 3D**), there was a significant increase in *Tgfβ1* expression in lungs treated with iPSCs vs. all other groups, P<0.001. Across all markers, there was a significant increase in gene expression between iPSC treated lungs vs. diPSC treated lungs, with the exception of *Il-6,* which was reduced*,* P<0.001. *Il-6* expression was significantly reduced in the iPSC treated group when compared to the normoxic group, P<0.01, and diPSC treated lungs, P<0.001 (**Figure 3D**). There was also a reduction in expression of *Il-6* in HBSS treated lungs compared to diPSC treated lungs, P<0.05. In regards to *Nfkb1*, expression was upregulated in HBSS treated lungs and the hyperoxic group compared to diPSCs, P<0.001. *Tgbf1* expression was increased in both the hyperoxic and HBSS groups compared to diPSCs (P<0.01-P<0.001). Expression was also significantly increased in HBSS treated samples vs. the normoxic group, P<0.05 (**Figure 3D**). There was no significant difference in expression across all markers between the hyperoxic and normoxic groups. The protein expression of the same set of markers, IL-6 and TGFβ1, and additionally MMP2- a matrix remodeling protein associated with fibrotic conditions, was confirmed by immunofluorescent staining in all treatment groups and controls (**Figure 4**). Cytosolic expression of MMP2 was evident along with TGFβ1 in all groups, with the highest intensity of staining seen in the hyperoxic tissue. All treatment groups also had positive staining for IL-6, with the exception of the vehicle control.

Isolation, characterization and delivery of exosomes derived from iPSCs and diPSCs

In order to assess the binding of exosomes to CD63/CD81 antibody conjugated beads, scanning electron microscopy was performed on samples revealing the presence of appropriately sized vesicles (**Figure 5A**). Exosomes derived from both iPSCs and diPSCs expressed the exosomal markers CD63 (72% and 80% respectively) and CD81 (both 100%) (**Figure 5C**) and were sorted prior to administration. Western Blot analysis of exosomes derived from iPSCs showed protein bands at 55 kDa (CD63) and 25 kDa (CD81) (**Figure 5B**).

The administration of sorted exosome bound beads to mice exposed to 14 days of hyperoxia revealed that the beads were detrimental to lungs. There was a significant difference in the MLI of the normoxic group compared to both iPSC and diPSC sorted beads (P< 0.01-P<0.001) (**Figure 5D**). There was also a significant difference between the bead only control and sorted iPSC and diPSCs (P< 0.001-P<0.01) (**Figure 5D**). Representative histology images revealed significant septal thickening and alveolar simplification in the bead control and iPSC and diPSC sorted beads (**Figure 5E**).

Discussion

New and effective treatments for bronchopulmonary dysplasia are lacking. Surfactant and corticosteroid administration are beneficial in the short-term for improving symptoms, however no current treatment is able to ameliorate hyperoxia-induced lung damage brought about by oxygen supplementation. Stem cells have shown promise as an alternative therapy to regenerate damaged tissue [42]. iPSCs are an attractive option due to their limitless expansion capability and potential for autologous derivation.

The present study evaluated the effectiveness of undifferentiated iPSCs and iPSCs differentiated to an alveolar-like phenotype in the amelioration of hyperoxia-induced lung damage in a mouse model.

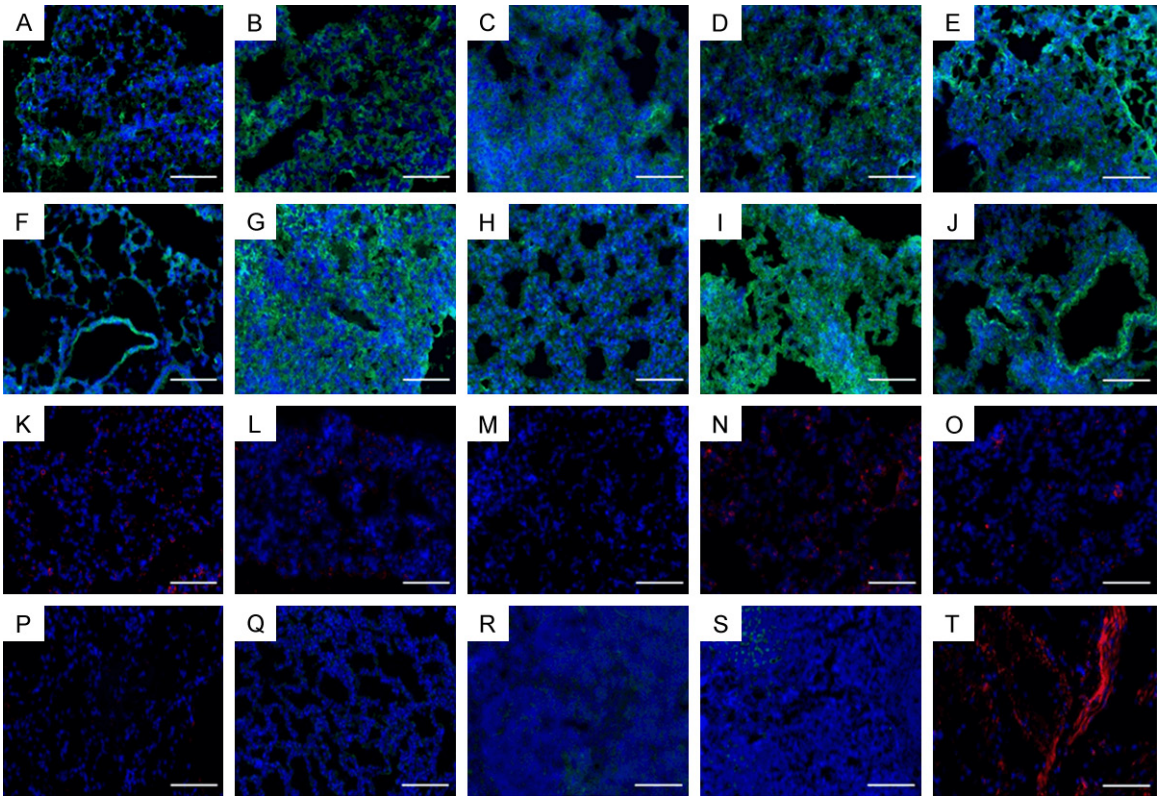

Figure 4. Representative immunofluorescent staining of mouse lungs 14 days after treatment, scale bars 50 μm. A-E. MMP2; F-J. TGFβ1; K-O. IL6; A, F, K. normoxia; B, G, L. hyperoxia; C, H, M. HBSS; D, I, N. iPSC; E, J, O. diPSC; P. Negative Goat Anti-Rat Control; Q. Negative Goat Anti-Rabbit Control; R. Positive Control TGFβ1; S. Positive Control MMP2; T. Positive Control IL-6.

In both 6 days and 14 days of hyperoxia exposure, the MLI of the hyperoxia and normoxia groups prior to treatment were significantly different from one other, validating the two models. There was no difference in the MLI of the vehicle treated lungs compared to the hyperoxia group, indicating that the vehicle had no effect on the model or influenced cell treatment. Additionally, a significant increase in MLI was observed in mice exposed to 6 and 14 days of 75% oxygen and administered induced pluripotent stem cells (iPSCs), when compared to the untreated hyperoxia group. Differentiated iPSC (diPSC) treated lungs exhibited a slight improvement in MLI when compared to the hyperoxia group after 6 and 14 days of O_2 exposure, however not to the same extent seen with iPSCs.

In order to further assess tissue regeneration post cell treatment, analysis of genes involved in inflammation (*Il-6, Tgfβ1, Nfkb1*) were analyzed. After 6 and 14 days of hyperoxia, gene expression of *Il-6 and Tgfβ1* in diPSC treated lungs 14 days' post treatment revealed that these cells were not as effective at mitigating the inflammatory response seen in hyperoxia when compared with iPSCs. *Tgfβ1* has been shown to act as an immune suppressor and plays a role in airway epithelial repair during acute lung injury [43-45]. At these time points, when compared to all treatment groups, expression in diPSC-treated lungs from the 14-day exposure was low, yet higher in the 6-day exposure. This indicates that the duration of hyperoxia exposure and the corresponding degree of injury leads to differences in transcriptional events related to tissue repair. The fact that *Tgfβ1* expression is relatively low in both exposures may partially explain the elevated *Il-6* expression also evident at the same time points. In comparison, iPSC treated lungs had significantly lower *Il-6* expression, indicating that the cells may possess anti-inflammatory properties. *Il-6* is a pleiotropic cytokine produced in response to inflammatory conditions [46] and causes ex-

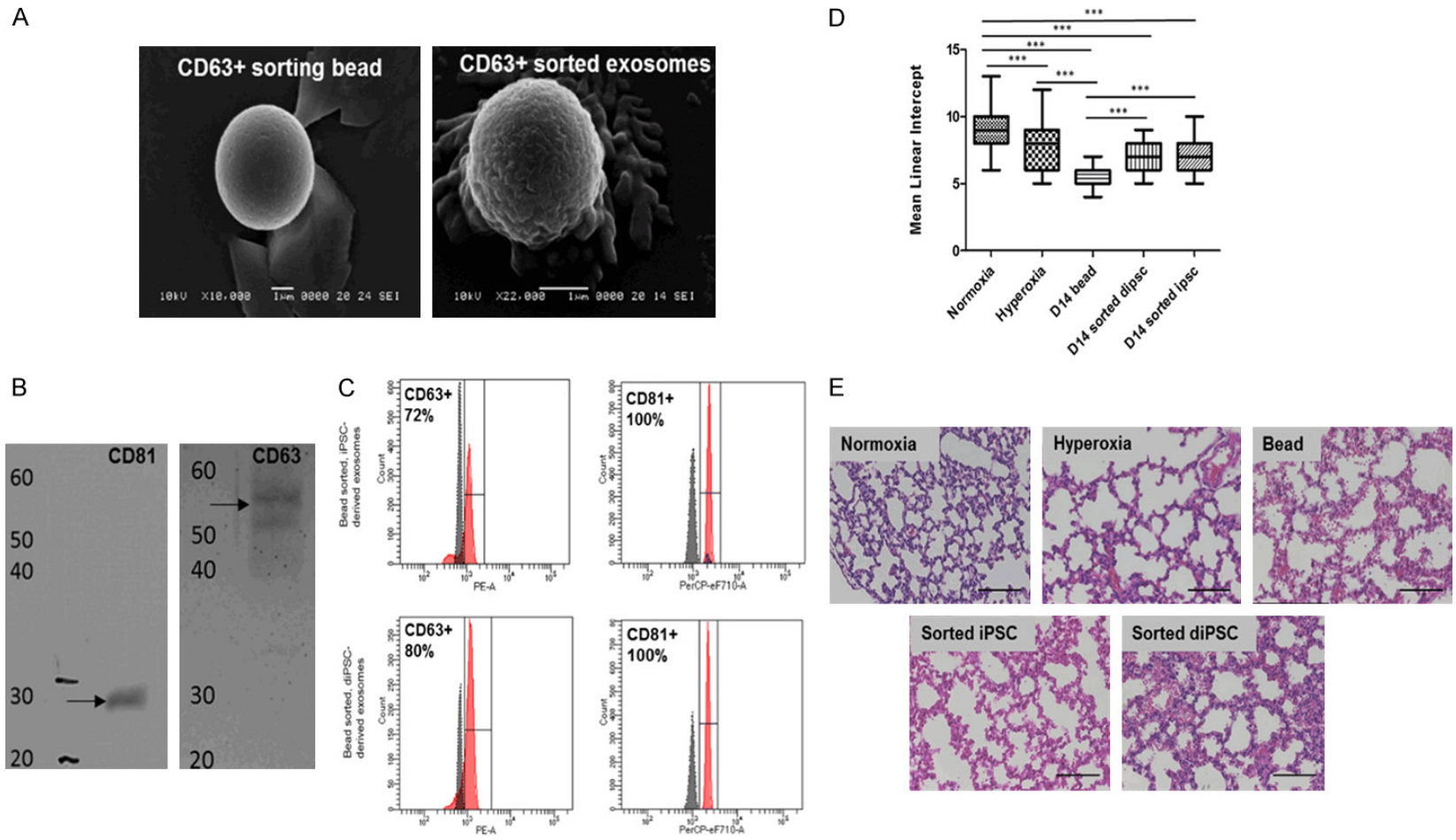

Figure 5. Characterization of exosomes derived from iPSCs and diPSCs. A. SEM analysis of CD63 + sorting beads with and without exosomes. B. Western blot analysis of exosomes derived from iPSCs. Exosomes isolated with CD81 sorting beads were positive for both CD81 (MW: 28 kDa) and CD63 (MW: 55 kDa) surface markers. C. FACS analysis of exosomes derived from both iPSCs and diPSCs and bound to CD63 and CD81 sorted beads. iPSC derived exosomes were positive for CD63 and CD81 surface markers (72% and 100%, respectively). diPSC derived exosomes were positive for CD63 and CD81 surface markers (80% and 100%, respectively). D. Mean linear intercept values for mice administered diPSC and iPSC derived exosomes bound to beads. Across all groups the statistically significant differences were seen in normoxia vs. hyperoxia, $P<0.001$ normoxia vs. D14 bead, $P<0.001$ normoxia vs. D14 sorted diPSC, $P<0.001$ normoxia vs. D14 sorted iPSC, $P<0.001$ hyperoxia vs. D14 bead, $P<0.001$ D14 bead vs. D14 sorted iPSC, $P<0.001$ D14 bead vs. D14 sorted diPSC, $P<0.001$. $P<0.01$. *$P<0.05$, **$P<0.01$, ***$P<0.001$ between indicated groups. E. Representative H + E staining of all groups, each image has the MLI closest to the group mean, scale bars 50 μm.

tensive damage to DNA and increases cell death regulator and angiogenic factor expression [47]. iPSCs have been shown to reduce the expression of pro-inflammatory cytokines such as *Il-6* when transplanted *in vivo* [48]. When comparing the immunogenicity and immunomodulatory properties of iPSCs to MSCs, one study found that MHC-mismatched iPSCs significantly reduced responder T-cell proliferation upon co-culture with MHC-mismatched leukocytes while MHC-mismatched MSCs did not [49]. Another study demonstrated that iPSCs were able to reduce the levels of pro-inflammatory cytokines and reduce neutrophil trafficking in lungs exposed to acute hyperoxic lung injury [20]. The exact mechanisms behind the immuno-modulatory capabilities of iPSCs have yet to be elucidated and further studies are needed to determine whether they lose their ability to mediate inflammatory responses once differentiated. This may explain why diPSC treated lungs exhibited increased *Il-6* expression and less morphologic repair overall compared to the iPSC-treated group. Surprisingly, in the 14-day exposure, HBSS returned gene expression to levels seen in the normoxic control, however morphologically this group was more similar to the hyperoxic control. This contradictory finding may partially be explained by differences in the way individual animals respond to lung injury at each time point. In addition, sampling of the whole lung to evaluate gene expression may lead to further inconsistencies due to the heterogeneity of the cells that make up the tissue overall.

Contrary to the function of *Tgfβ1*, *Nfkb1* regulates immune response to infection [50]. The differential expression of *Nfkb1* across cell types and O_2 exposures indicate that *Nfkb1* expression, along with expression of *Tgfβ1* and *Il-6* in the vehicle control, will need to be closely monitored at more frequent time points to assess trends. Gender-specific differences in terms of hyperoxic injury and how this affects relative gene expression of inflammatory markers will also need to be investigated.

Representative immunofluorescent staining of treated lungs exposed to 14 days of hyperoxia confirmed the presence of TGFβ1 and IL-6 in all groups, including MMP2, a matrix metalloproteinase that contributes to lung injury [51]. The hyperoxic control appeared to have the greatest intensity of staining across all proteins. TGFβ1 staining in iPSC-treated lungs was also increased compared to all other groups, which corroborated the findings from the gene expression analysis. Any further correlation of protein expression levels to the gene data are difficult to assess, which may be due to the differences in which the tissue was processed for each analysis (whole vs. section). Nonetheless, it is clear that expression of these inflammatory markers is evident across all groups.

Based solely on histomorphometric analysis of lung samples, iPSCs had an impact on repairing lung damage. The gene data suggests that iPSCs possess immunomodulatory properties, which impacts lung morphology by reducing the inflammatory environment in hyperoxic conditions. Our study investigated only three genes for the assessment of tissue repair, however a recent paper showed that the omics of bronchopulmonary dysplasia is very complex and involves the dysregulation of over 300 genes [52]. Analysis of a small number of genes gives a limited picture, and more will need to be evaluated to determine the full extent of tissue repair initiated by iPSC treatment.

Our findings, similar to those of a previous study, established that diPSCs are able attenuate the response to hyperoxia, however they do not fully reverse the damage [53].

In contrast, iPSCs were highly effective at ameliorating the negative effects of hyperoxic conditions on lung tissue rendering differentiation to an alveolar phenotype unnecessary. The primary obstacle to their clinical translation is their teratogenic potential upon *in vivo* administration [54]. The adaptation of iPSCs into a cell-free therapeutic using their secreted extracellular vesicles would potentially alleviate many of these concerns [55-58]. Exosomes are small, secreted vesicles (30-150 nm) that are found in several different tissues of the body and mediate intercellular signaling and also the transport of materials [59]. They originate from multivesicular bodies and have been shown to possess regenerative properties mediated through the release of paracrine signals [60-64]. They are easy to store, relatively inexpensive to produce and possess a lower immunogenic response than their cellular counterparts. Furthermore, there is no concern for engraftment within the location they are administered,

eliminating concerns seen with viable cells [65]. Exosomes derived from iPSCs and diPSCs, were isolated from each cell type in order to assess their therapeutic potential. Our preliminary findings demonstrate the feasibility of isolating exosome populations expressing high levels of appropriate markers. When administered to mice exposed to 14 days of hyperoxia, it was evident that the exosomes bound to magnetic beads caused further damage to the lungs than hyperoxia alone. However, mice that received exosome/bead complexes suffered less damage than mice receiving just beads indicating that the exosomes may have had some beneficial effect. Future studies will focus on methods to dissociate bead bound exosomes before administration, along with determination of therapeutic dosage necessary to elicit lung repair. In conclusion, this study demonstrates the capability of iPSCs to reverse hyperoxia-induced lung damage in a mouse model and highlights their potential immunomodulatory properties. Future studies will investigate whether exosomes derived from iPSCs can exert the same effect as their cellular counterpart and adapt them as a cell-free therapeutic alternative for BPD prevention. This would pave the way for novel therapies for treatment of premature infants suffering from chronic respiratory illnesses.

Acknowledgements

We would like to acknowledge the assistance with our project from the UConn Health Research Histology and Flow Cytometry core facilities. We would also like to acknowledge the assistance of our animal facility staff with husbandry of our animals.

Disclosure of conflict of interest

None.

Address correspondence to: Christine Finck, University of Connecticut Health Center, 263 Farmington Ave, Farmington, CT, USA. Tel: 860-545-9634; Fax: 860-545-8511; E-mail: Cfinck@connecticutchildrens.org

References

[1] Kalikkot Thekkeveedu R, Guaman MC and Shivanna B. Bronchopulmonary dysplasia: a review of pathogenesis and pathophysiology. Resp Med 2017; 132: 170-177.

[2] Perrone S, Santacroce A, Longini M, Proietti F, Bazzini F and Buonocore G. The free radical diseases of prematurity: from cellular mechanisms to bedside. Oxid Med Cell Longev 2018; 2018: 7483062.

[3] Wang J and Dong W. Oxidative stress and bronchopulmonary dysplasia. Gene 2018; 678: 177-183.

[4] Principi N, Di Pietro DM and Esposito S. Bronchopulmonary dysplasia: clinical aspects and preventive and therapeutic strategies. J Transl Med 2018; 16: 1-13.

[5] DeMauro SB. The impact of bronchopulmonary dysplasia on childhood outcomes. Clin Perinatol 2018; 45: 439-452.

[6] Möbius MA and Thébaud B. Stem cells and their mediators - next generation therapy for bronchopulmonary dysplasia. Front Med 2015; 2: 1-12.

[7] O'Reilly M and Thébaud B. Cell-based therapies for neonatal lung disease. Cell Tissue Res 2017; 367: 737-745.

[8] Thébaud B. Stem cell-based therapies in neonatology: a new hope. Arch Dis Child Fetal Neonatal Ed 2018; 103: F583-F588.

[9] Álvarez-Fuente M, Arruza L, Lopez-Ortego P, Moreno L, Ramírez-Orellana M, Labrandero C, González Á, Melen G and Cerro MJD. Off-label mesenchymal stromal cell treatment in two infants with severe bronchopulmonary dysplasia: clinical course and biomarkers profile. Cytotherapy 2018; 20: 1337-1344.

[10] Liang X, Ding Y, Zhang Y, Tse HF and Lian Q. Paracrine mechanisms of mesenchymal stem cell-based therapy: current status and perspectives. Cell Transplant 2014; 23: 1045-1059.

[11] Park WS, Ahn SY, Sung SI, Ahn JY and Chang YS. Strategies to enhance paracrine potency of transplanted mesenchymal stem cells in intractable neonatal disorders. Ped Res 2017; 83: 214-222.

[12] Pierro M, Ionescu L, Montemurro T, Vadivel A, Weissmann G, Oudit G, Emery D, Bodiga S, Eaton F, Péault B, Mosca F, Lazzari L and Thébaud B. Short-term, long-term and paracrine effect of human umbilical cord-derived stem cells in lung injury prevention and repair in experimental bronchopulmonary dysplasia. Thorax 2013; 68: 475-484.

[13] Fitzsimmons REB, Mazurek MS, Soos A and Simmons CA. Mesenchymal stromal/stem cells in regenerative medicine and tissue engineering. Stem Cells Int 2018; 2018: 8031718.

[14] Odabas S, Elçin AE and Elçin YM. Isolation and characterization of mesenchymal stem cells. bone marrow and stem cell transplantation. Methods Mol Biol 2014; 1109: 47-63.

[15] Augustine S, Avey MT, Harrison B, Locke T, Ghannad M, Moher D and Thébaud B.

Mesenchymal stromal cell therapy in bronchopulmonary dysplasia: systematic review and meta-analysis of preclinical studies. Stem Cells Trans Med 2017; 6: 2079-2093.
[16] Chang YS, Choi SJ, Ahn SY, Sung DK, Sung SI, Yoo HS, Oh WI and Park WS. Timing of umbilical cord blood derived mesenchymal stem cells transplantation determines therapeutic efficacy in the neonatal hyperoxic lung injury. PLoS One 2013; 8: 1-11.
[17] Phinney DG. Functional heterogeneity of mesenchymal stem cells: implications for cell therapy. J Cell Biochem 2012; 113: 2806-2812.
[18] Durbin MD, Cadar AG, Chun YW and Hong CC. Investigating pediatric disorders with induced pluripotent stem cells. Ped Res 2018; 84: 499-508.
[19] Qi SD, Smith PD and Choong PF. Nuclear reprogramming and induced pluripotent stem cells: a review for surgeons. ANZ J Surg 2014; 84: 417-423.
[20] Liu YY, Li LF, Fu JY, Kao KC, Huang CC, Chien Y, Liao YW, Chiou SH and Chang YL. Induced pluripotent stem cell therapy ameliorates hyperoxia-augmented ventilator-induced lung injury through suppressing the Src pathway. PLoS One 2014; 9: e109953.
[21] Liu YY, Li LF, Yang CT, Lu KH, Huang CC, Kao KC and Chiou SH. Suppressing NF-κB and NKRF pathways by induced pluripotent stem cell therapy in mice with ventilator-induced lung injury. PLoS One 2013; 8: e66760.
[22] Dannenmann B, Lehle S, Hildebrand DG, Kübler A, Grondona P, Schmid V, Holzer K, Fröschl M, Essmann F, Rothfus O and Schulze-Osthoff K. High glutathione and glutathione peroxidase-2 levels mediate cell-type-specific DNA damage protection in human induced pluripotent stem cells. Stem Cell Rep 2015; 4: 886-898.
[23] Li LF, Liu YY, Yang CT, Chien Y, Twu NF, Wang ML, Wang CY, Huang CC, Kao KC, Hsu HS, Wu CW and Chiou SH. Improvement of ventilator-induced lung injury by IPS cell-derived conditioned medium via inhibition of PI3K/Akt pathway and IP-10-dependent paracrine regulation. Biomaterials 2013; 34: 78-91.
[24] Armstrong L, Tilgner K, Saretzki G, Atkinson SP, Stojkovic M, Moreno R, Przyborski S and Lako M. Human induced pluripotent stem cell lines show stress defense mechanisms and mitochondrial regulation similar to those of human embryonic stem cells. Stem Cells 2010; 28: 661-673.
[25] Green MD, Chen A, Nostro MC, d'Souza SL, Schaniel C, Lemischka IR, Gouon-Evans V, Keller G and Snoeck HW. Generation of anterior foregut endoderm from human embryonic and induced pluripotent stem cells. Nat Biotechnol 2011; 29: 267-272.
[26] Huang SX, Islam MN, O'Neill J, Hu Z, Yang YG, Chen YW, Mumau M, Green MD, Vunjak-Novakovic G, Bhattacharya J and Snoeck HW. Efficient generation of lung and airway epithelial cells from human pluripotent stem cells. Nat Biotechnol 2014; 32: 84-91.
[27] Ninomiya H, Mizuno K, Terada R, Miura T, Ohnuma K, Takahashi S, Asashima M and Michiue T. Improved efficiency of definitive endoderm induction from human induced pluripotent stem cells in feeder and serum-free culture system. In Vitro Cell Dev Biol Anim 2015; 51: 1-8.
[28] Huang SXL, Green MD, de Carvalho AT, Mumau M, Chen YW, D'Souza SL and Snoeck HW. The in vitro generation of lung and airway progenitor cells from human pluripotent stem cells. Nat Protoc 2015; 10: 413-425.
[29] Barkauskas CE, Cronce MJ, Rackley CR, Bowie EJ, Keene DR, Stripp BR, Randell SH, Noble PW and Hogan BL. Type 2 alveolar cells are stem cells in adult lung. J Clin Invest 2013; 123: 3025-3036.
[30] Collins JJ and Thébaud B. Progenitor cells of the distal lung and their potential role in neonatal lung disease. Birth Defects Res A Clin Mol Teratol 2014; 100: 217-226.
[31] Martin TR and Frevert CW. Innate immunity in the lungs. Proc Am Thorac Soc 2005; 2: 403-411.
[32] Buckley S, Shi W, Carraro G, Sedrakyan S, Da Sacco S, Driscoll BA, Perin L, De Filippo RE and Warburton D. The milieu of damaged alveolar epithelial type 2 cells stimulates alveolar wound repair by endogenous and exogenous progenitors. Am J Resp Cell Mol 2011; 45: 1212-1221.
[33] Mitchell A, Wanczyk H, Jensen T and Finck C. Assessment of iPSC teratogenicity throughout directed differentiation toward an alveolar-like phenotype. Differentiation 2019; 105: 45-53.
[34] Mitchell A, Drinnan CT, Jensen T and Finck C. Production of high purity alveolar-like cells from iPSCs through depletion of uncommitted cells after AFE induction. Differentiation 2017; 96: 62-69.
[35] Crisanti MC, Koutzaki SH, Mondrinos MJ, Lelkes PI and Finck CM. Novel methods for delivery of cell-based therapies. J Surg Res 2008; 146: 3-10.
[36] Muñoz-Barrutia A, Ceresa M, Artaechevarria X, Montuenga LM and Ortiz-de-Solorzano C. Quantification of lung damage in an elastase-induced mouse model of emphysema. Int J Biomed Imag 2012; 2012: 734734.
[37] Bhandari V. Hyperoxia-derived lung damage in preterm infants. Semin Fetal Neonatal Med 2010; 15: 223-229.
[38] Lesage F, Jimenez J, Toelen J and Deprest J. Preclinical evaluation of cell-based strategies

to prevent or treat bronchopulmonary dysplasia in animal models: a systematic review. J Matern Fetal Neonatal Med 2018; 31: 958-966.
[39] Bhandari V and Elias JA. Cytokines in tolerance to hyperoxia-induced injury in the developing and adult lung. Free Radical Bio Med 2006; 41: 4-18.
[40] Monz D, Tutdibi E, Mildau C, Shen J, Kasoha M, Laschke MW, Roolfs T, Schmiedl A, Tschernig T, Bieback K and Gortner L. Human umbilical cord blood mononuclear cells in a double-hit model of bronchopulmonary dysplasia in neonatal mice. PLoS One 2013; 8: e74740.
[41] Alejandre-Alcázar MA, Kwapiszewska G, Reiss I, Amarie OV, Marsh LM, Sevilla-Pérez J, Wygrecka M, Eul B, Köbrich S, Hesse M, Schermuly RT, Seeger W, Eickelberg O and Morty RE. Hyperoxia modulates TGF-β/BMP signaling in a mouse model of bronchopulmonary dysplasia. Am J Physiol Lung Cell Mol Physiol 2007; 292: 537-549.
[42] Kang M and Thébaud B. Stem cell biology and regenerative medicine for neonatal lung diseases. Pediatr Res 2017; 83: 291-297.
[43] Han G, Li F, Singh TP, Wolf P and Wang XJ. The pro-inflammatory role of TGFβ1: a paradox? Int J Biol Sci 2012; 8: 228-235.
[44] Thomas BJ, Kan-O K, Loveland KL, Elias JA and Bardin PG. In the shadow of fibrosis: innate immune suppression mediated by transforming growth factor-β. Am J Resp Cell Mol 2016; 55: 759-766.
[45] Jolly MK, Ward C, Eapen MS, Myers S, Hallgren O, Levine H and Sohal SS. Epithelial-mesenchymal transition, a spectrum of states: role in lung development, homeostasis, and disease. Dev Dynam 2018; 247: 346-358.
[46] Waxman AB and Kolliputi N. IL-6 protects against hyperoxia-induced mitochondrial damage via Bcl-2-induced Bak interactions with mitofusins. Am J Resp Cell Mol 2009; 41: 385-396.
[47] Choo-Wing R, Nedrelow JH, Homer RJ, Elias JA and Bhandari V. Developmental differences in the responses of IL-6 and IL-13 transgenic mice exposed to hyperoxia. Am J Physiol Lung Cell Mol Physiol 2007; 293: L142-L150.
[48] Qin J, Ma X, Qi H, Song B, Wang Y, Wen X, Wang QM, Sun S, Li Y, Zhang R, Liu X, Hou H, Gong G and Xu Y. Transplantation of induced pluripotent stem cells alleviates cerebral inflammation and neural damage in hemorrhagic stroke. PLoS One 2015; 10: e0129881.
[49] Schnabel LV, Abratte CM, Schimenti JC, Felippe MJB, Cassano JM, Southard TL, Cross JA and Fortier LA. Induced pluripotent stem cells have similar immunogenic and more potent immunomodulatory properties compared with bone marrow-derived stromal cells in vitro. Regen Med 2014; 9: 621-635.
[50] Cartwright T, Perkins ND and Wilson C. NFKB1: a suppressor of inflammation, ageing and cancer. FEBS J 2016; 283: 1812-1822.
[51] Villalta, PC, Rocic P and Townsley MI. Role of MMP2 and MMP9 in TRPV4-induced lung injury. Am J Physiol Lung Cell Mol Physiol 2014; 307: 652-659.
[52] Shrestha AK, Gopal VYN, Menon RT, Hagan JL, Huang S and Shivanna B. Lung omics signatures in a bronchopulmonary dysplasia and pulmonary hypertension-like murine model. Am J Physiol Lung Cell Mol Physiol 2018; 315: L734-L741.
[53] Shafa M, Ionescu LI, Vadivel A, Collins JJP, Xu L, Zhong S, Kang M, de Caen G, Daneshmand M, Shi J, Fu KZ, Qi A, Wang Y, Ellis J, Stanford WL and Thébaud B. Human induced pluripotent stem cell-derived lung progenitor and alveolar epithelial cells attenuate hyperoxia-induced lung injury. Cytotherapy 2018; 20: 108-125.
[54] Deng J, Zhang Y, Xie Y, Zhang L and Tang P. Cell transplantation for spinal cord injury: tumorigenicity of induced pluripotent stem cell-derived neural stem/progenitor cells. Stem Cells Int 2018; 2018: 5653787.
[55] Lesage F and Thébaud B. Nanotherapies for micropreemies: stem cells and the secretome in bronchopulmonary dysplasia. Semin Perinatol 2018; 42: 453-458.
[56] Porzionato A, Zaramella P, Dedja A, Guidolin D, Van Wemmel K, Macchi V, Jurga M, Perilongo G, De Caro R, Baraldi E and Muraca M. Intratracheal administration of mesenchymal stem-cell-derived extracellular vesicles reduced lung injury in a rat model of bronchopulmonary dysplasia. Am J Physiol Lung Cell Mol Physiol 2019; 16; 6-19.
[57] Willis GR, Kourembanas S and Mitsialis SA. Therapeutic applications of extracellular vesicles: perspectives from newborn medicine. Methods Mol Biol 2017; 1660: 409-432.
[58] Gazdhar A, Ravikumar P, Pastor J, Heller M, Ye J, Zhang J, Moe OW, Geiser T and Hsia CCW. Alpha-klotho enrichment in induced pluripotent stem cell secretome contributes to antioxidative protection in acute lung injury. Stem Cells 2018; 36: 616-625.
[59] Jing H, He X and Zheng X. Exosomes and regenerative medicine: state of the art and perspectives. Transl Res 2018; 196: 1-16.
[60] Willis GR, Fernandez-Gonzalez A, Anastas J, Vitali SH, Liu X, Ericsson M, Kwong A, Mitsialis SA and Kourembanas S. Mesenchymal stromal cell exosomes ameliorate experimental bronchopulmonary dysplasia and restore lung

function through macrophage immunomodulation. Am J Resp Crit Care 2018; 197: 104-116.
[61] Tan KS, Choi H, Jiang X, Yin L, Seet JE, Patzel V, Engelward BP and Chow VT. Micro-RNAs in regenerating lungs: an integrative systems biology analysis of murine influenza pneumonia. BMC Genomics 2014; 15: 587-587.
[62] Vaporidi K, Vergadi E, Kaniaris E, Hatziapostolou M, Lagoudaki E, Georgopoulos D, Zapol WM, Bloch KD and Iliopoulos D. Pulmonary microRNA profiling in a mouse model of ventilator-induced lung injury. Am J Physiol Lung Cell Mol Physiol 2012; 303: 199-207.
[63] Oudina K, Paquet J, Moya A, Massourides E, Bensidhoum M, Larochette N, Deschepper M, Pinset C and Petite H. The paracrine effects of human induced pluripotent stem cells promote bone-like structures via the upregulation of BMP expression in a mouse ectopic model. Sci Rep 2018; 8: 1-10.
[64] Gartz M and Strande JL. Examining the paracrine effects of exosomes in cardiovascular disease and repair. J Am Heart Assoc 2018; 7: 1-13.
[65] Bjørge IM, Kim SY, Mano JF, Kalionis B and Chrzanowski W. Extracellular vesicles, exosomes and shedding vesicles in regenerative medicine - a new paradigm for tissue repair. Biomater Sci 2018; 6: 60-78.

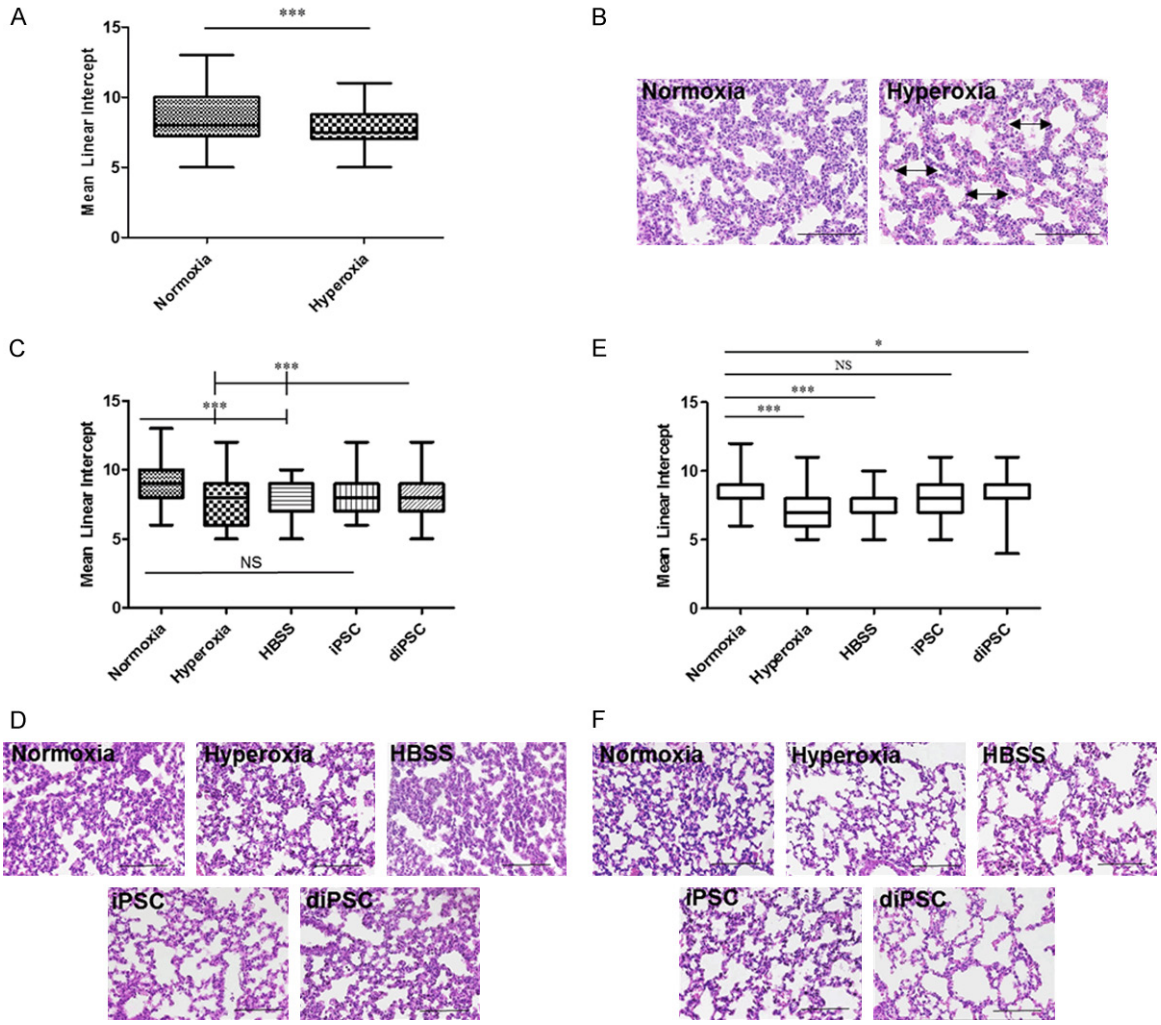

Figure S1. Histomorphometric data of C57 BL/6 mouse lungs following 6 days of hyperoxia induced lung damage. A, C, E. Mean linear intercept values for all groups. The MLI was calculated by counting and then averaging the linear intercepts of alveolar walls from each image (6 images/group). A. Post-natal Day 7. There was a statistically significant difference between normoxia vs. hyperoxia, $P<0.001$. C. 7 days post cell treatment. Across all groups the statistically significant differences were seen in normoxia vs. hyperoxia, $P<0.001$ normoxia vs. HBSS, $P<0.001$ hyperoxia vs. diPSC, $P<0.001$. E. 14 days post cell treatment. Across all groups the statistically significant differences were seen in normoxia vs. hyperoxia, $P<0.001$ normoxia vs. HBSS, $P<0.001$ normoxia vs. diPSC, $P<0.05$ normoxia vs. iPSC, no statistically significant difference seen between the two groups. *$P<0.05$, **$P<0.01$, ***$P<0.001$ between the indicated groups. B, D, F. Representative H + E staining of all groups, scale bars 50 μm. B. Post-natal Day 7. The presence of alveolar simplification is indicated by double-sided arrows and septal thickening by single-sided arrows. D. 7 days post cell treatment. F. 14 days post cell treatment.

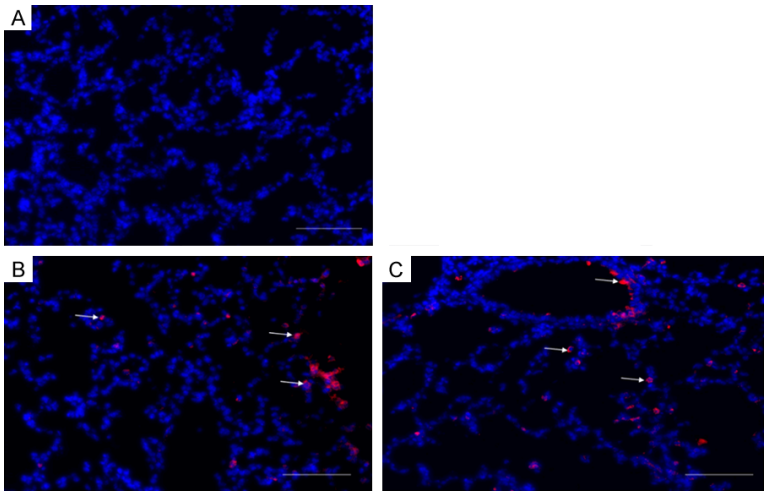

Figure S2. CellBrite™ Fix Membrane Staining of iPSCs delivered intraorally to P15 neonatal mice, scale bars 50 μm. A. Negative Control. B, C. Localization of stained iPSCs within the alveoli and airways of lungs 1 hour post administration.